

Article

Coal-Based Reduction and Magnetic Separation Behavior of Low-Grade Vanadium-Titanium Magnetite Pellets

Gongjin Cheng ^{1,*}, Zixian Gao ¹, Mengyang Lv ¹, He Yang ^{1,2} and Xiangxin Xue ^{1,2,*}

¹ School of Metallurgy, Northeastern University, Shenyang 110819, China; gaozixian001@163.com (Z.G.); lvmengyang001@163.com (M.L.); yangh@smm.neu.edu.cn (H.Y.)

² Liaoning Key Laboratory of Recycling Science for Metallurgical Resources, Shenyang 110819, China

* Correspondence: successking123@gmail.com (G.C.); xuexx@mail.neu.edu.cn (X.X.);
Tel.: +86-24-8368-4086 (G.C.); +86-24-8368-7719 (X.X.)

Academic Editor: Shifeng Dai

Received: 26 March 2017; Accepted: 18 May 2017; Published: 23 May 2017

Abstract: Coal-based reduction and magnetic separation behavior of low-grade vanadium-titanium magnetite pellets were studied in this paper. It is found that the metallization degree increased obviously with an increase in the temperature from 1100 °C to 1400 °C. The phase composition transformation was specifically analyzed with X-ray diffraction (XRD). The microscopic examination was carried out with scanning electron microscopy (SEM), and the element composition and distribution were detected with energy dispersive spectroscopy (EDS). It is observed that the amounts of metallic iron particles obviously increased and the accumulation and growing tendency were gradually facilitated with the increase in the temperature from 1100 °C to 1400 °C. It is also found that the titanium oxides were gradually reduced and separated from ferrum-titanium oxides during reduction. In addition, with increasing the temperature from 1200 °C to 1350 °C, silicate phases, especially calcium silicate phases that were transformed from calcium ferrite at 1100 °C, were observed and gradually aggregated. However, at 1400 °C some silicate phases infiltrated into metallic iron, as it appears that the carbides, especially TiC, could probably contribute to the sintering phenomenon becoming serious. The transformation behavior of valuable elements was as follows: $\text{Fe}_2\text{VO}_4 \rightarrow \text{VO} \rightarrow \text{V} \rightarrow \text{VC}$; $\text{FeTiO}_3 (\rightarrow \text{FeTi}_2\text{O}_5) \rightarrow \text{TiO}_2 \rightarrow \text{TiC}$; $\text{FeCr}_2\text{O}_4 \rightarrow \text{Cr} \rightarrow \text{CrC}$; $\text{FeTiO}_3 (\rightarrow \text{FeTi}_2\text{O}_5) \rightarrow \text{Fe}_{0.5}\text{Mg}_{0.5}\text{Ti}_2\text{O}_5$; $(\text{Fe}_3\text{O}_4/\text{FeTiO}_3 \rightarrow) \text{FeO} \rightarrow \text{Mg}_{0.77}\text{Fe}_{0.23}\text{O}$. Through the magnetic separation of coal-based reduced products, it is demonstrated that the separation of Cr, V, Ti, and non-magnetic phases can be preliminarily realized.

Keywords: low-grade vanadium-titanium magnetite; pellets; coal-based reduction; magnetic separation behavior

1. Introduction

As it is known, there are more than 10 billion tons of vanadium-titanium magnetite ores in China and these ores are mainly distributed in the Panxi district in Sichuan Province, Chengde district in Hebei Province, and Maanshan district in Anhui Province [1,2]. However, in recent years, one special kind of vanadium-titanium magnetite ore in a certain area in Liaoning Province has been found, and these special mineral resources are low-grade vanadium-titanium magnetite (LGVTM) [3]. With the considerable decrease of high-grade ores, it is necessary to utilize these low-grade ores, and studies of these special LGVTM have been scarcely reported. Thus, it is of great necessity to carry out studies on these unique mineral resources.

Vanadium-titanium magnetite, as one kind of multi-mineral iron ore, is rich in valuable elements, including Fe, V, Ti, Cr, etc., and is developing significant value [1–7]. Compared with

the vanadium-titanium magnetite in Panxi district and Chengde district, present investigated vanadium-titanium magnetite has the characteristics of lower iron, higher titanium, and higher vanadium [1,2,8–10]. It is promising to utilize these special mineral resources by a non-blast furnace (BF) process. Coal-based direct reduction, followed by magnetic separation, as one special non-BF technique, has the advantages of a relatively much shorter process, its easy operation process, lower energy consumption, and lower production price for the process since the coal replaces coke [9,11]. It is, therefore, rewarding to investigate the coal-based direct reduction–magnetic separation of low-grade vanadium-titanium magnetite to improve the utilization efficiency of Fe, and especially of V, Ti, and Cr.

For the coal-based direct reduction process, considerable studies have been done for hematite ores [11–16], in which the following process of magnetic separation has also been reported by Yu et al.'s study [11]. Due to the depletion of high-grade hematite ores, the utilization of magnetite ores has been attempted [9,15,17–23]. For ordinary vanadium-titanium magnetite, previous work can be found in [8,9,20–23]. Jung [20] has investigated the effects of CaO/CaCO₃ on the carbothermic reduction of titanomagnetite ores. Jung [21,22] has also investigated the effects of the content and particle size of char in the composite on the carbothermic reduction of titanomagnetite at 1100 °C and the evaluation of isothermal reduction progress of raw titanomagnetite and char composite by thermogravimetry at 1200 °C. Hu et al. [23] researched the effect of Fe-Si on the carbothermic reduction of Panzhihua titanomagnetite concentrates under an argon atmosphere by isothermal experiments at 1350 °C and non-isothermal experiments in the temperature range from room temperature to 1450 °C, respectively. Sun [8] has researched the solid state reduction of titanomagnetite concentrate in Panxi district with graphite. Chen [9] has analyzed the metalizing reduction and magnetic separation of vanadium titanomagnetite (*TFe*: 53.91 wt %; V₂O₅: 0.52 wt %; TiO₂: 13.03 wt %) in Panxi district based on hot briquetting. However, the coal-based direct reduction on LGVTM has been elusive, let alone for the following process of magnetic separation. Consequently, it is important to carry out the present study.

Due to the researching margin of LGVTM and the promising direct reduction–magnetic separation technique, in this study, the coal-based reduction and magnetic separation behavior of low-grade vanadium-titanium magnetite pellets (LGVTMP) were studied. Qualified LGVTMP with suitable C/O (fixed carbon/oxygen) were firstly prepared, and the effect of the reduction temperature on the metallization degree, iron recovery rate, transformation behavior, and pattern of V, Ti, and Cr was studied. The phase composition transformation, microstructure analysis and micro-area composition were also investigated with different characterization means, including inductively coupled plasma–atomic emission spectroscopy (ICP-AES), X-ray fluorescence (XRF), X-ray diffraction (XRD), scanning electron microscope–energy dispersive spectroscopy (SEM-EDS), whose parameters are described in the experimental section.

2. Experimental

2.1. Experimental Materials

In the present study, LGVTMP were prepared by LGVTM, coal and mixed with 2% bentonite (binders). The ratio between LGVTM and the coal was calculated according to Equation (1):

$$C/O = \frac{(m_{coal} \times w_C) / M_C}{[m_{ore} \times (w_{O,Fe_2O_3} + w_{O,FeO})] / M_O} \quad (1)$$

where m_{coal} is the mass of reducing coal (g), m_{ore} is the mass of LGVTM (g), w_C is the fixed carbon percent of reducing coal (wt %), w_{O,Fe_2O_3} is the oxygen percent of Fe₂O₃ (wt %), $w_{O,FeO}$ is the oxygen percent of FeO (wt %), M_C is the molar mass of C (g/mol), M_O is the molar mass of O (g/mol), and the C/O of experimental coal-based pellets was 1.2. The LGVTM, whose size proportion of less than 0.074 mm was about 67%, was from northwestern district in Liaoning Province, and the chemical composition and phase composition are shown in Table 1 and Figure 1, respectively. The main Ti-bearing, V-bearing, and Cr-bearing phases are mainly FeTiO₃, Fe₂VO₄, and FeCr₂O₄. Examining the

XRD pattern, the interplanar crystal spacing (d-spacing) also exhibited above, or in close proximity to, the phase symbol, and the unit of d-spacing is Å (hereinafter suitable for XRD figures). Figure 2 presents a SEM image of LGVTM and the corresponding EDS analyses of different areas, from which it is found that areas 1, 2, and 4 were ilmenite, magnetite, and gangue phases. The coal size was less than 0.074 mm, and the chemical composition is shown in Table 2.

Table 1. Chemical composition of LGVTM (wt %).

TFe	FeO	V	TiO ₂	Cr ₂ O ₃	CaO	SiO ₂	MgO	Al ₂ O ₃	P	S
43.75	18.4	0.91	21.54	0.13	3.52	7.00	0.70	1.83	0.002	0.022

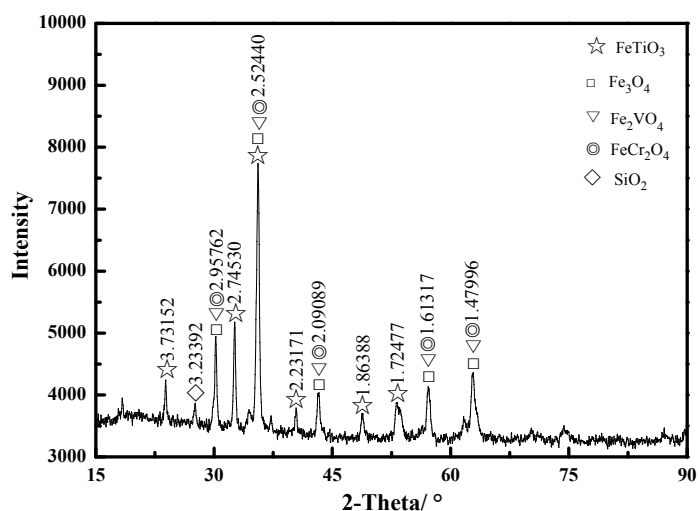


Figure 1. XRD pattern of LGVTM.

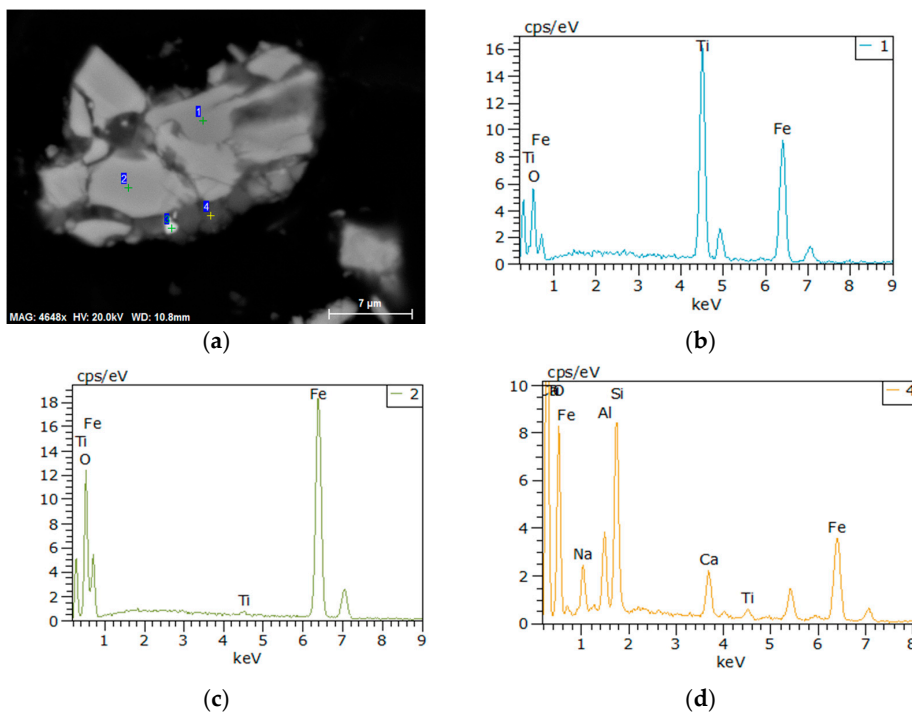


Figure 2. SEM image of LGVTM and corresponding EDS analyses of areas 1, 2, and 4: (a) SEM image of LGVTM; (b) EDS analysis of area 1; (c) EDS analysis of area 2; (d) EDS analysis of area 4.

Table 2. Proximate analysis of coal (wt %).

Fixed Carbon	Ash	Volatile Matter	Sulfur (S)
64.23	7.06	22.85	0.41

2.2. Experimental Methods

Present coal-based reduction–magnetic separation experiments mainly consist of the material calculation, material mixing, pelletizing, reduction roasting, reduced product cooling, sample preparation, magnetic separation, analysis, and characterization. Firstly, weighed LGVTM, coal, and bentonite were mixed in the mixing tank using a ball grinding mill for more than 5 h, in which the materials were ground further. Secondly, LGVTMP, with appropriate amount of water, were prepared using a disc balling machine. After drying in the oven for more than 5 h, 30 g of LGVTMP were put in each graphite crucible and small coals of 0.8–3 mm size were filled around the pellets. Then the pellets were roasted in the high-temperature resistance furnace (KJ-A1700-12LZ, Kejia Furnace Co. Ltd., Tianjin, China) with a suitable temperature regime, and Ar gas was employed to prevent the oxidation of the coal-based pellets. The reduction temperature was in the range of 1100–1400 °C and the reduction time was one hour. After reduction, the reduced products were cooled to room temperature by burying coal powders around the graphite crucible to prevent air from oxidizing the products. Then the reduced pellet products were ground for 3 min by the sampling machine (2MZ-100; Nanchang Hengshun Chemical Equipment Manufacturing Co. Ltd., Nanchang, China), and the ground reduced products were all less than 0.074 mm and magnetically separated (XCGS-φ50; Instrument Factory of Tianjin Hualian Mining, Tianjin, China) with different magnetic field intensities. After magnetic separation, different magnetic products and non-magnetic products were obtained.

The chemical analyses of reduced LGVTMP, magnetic and non-magnetic products were conducted by X-ray fluorescence (XRF, ZSXPrimus II; Rigaku, Tokyo, Japan) and inductively coupled plasma–atomic emission spectroscopy (ICP-AES, Optima 8300DV; PerkinElmer, Waltham, MA, USA). The phase compositions of reduced pellets, and magnetic and non-magnetic products were analyzed by X-ray diffraction (XRD, X' Pert Pro; PANalytical, Almelo, The Netherlands) with Cu K α radiation ($\lambda = 1.5406 \text{ \AA}$), and the microstructure, element compositions, and distributions of the reduced pellet products prepared with polished section were examined by scanning electron microscope–energy dispersive spectroscopy (SEM-EDS, Ultra Plus; Carl Zeiss GmbH, Jena, Germany), for which the type of imaging used back-scattered electrons.

3. Results and Discussion

3.1. Metallization Degree

Figure 3 shows the typical results of the metallization degree of the coal-based LGVTMP at 1100–1400 °C. The metallization degree is calculated according to Equation (2):

$$M = [w(MFe)/w(TFe)] \times 100\% \quad (2)$$

where M is the metallization degree (%), $w(MFe)$ is the mass percent of the metallic iron in reduced pellet products (%), $w(TFe)$ is the mass percent of the total ferrum in reduced pellet products (%). It is found that the metallization degree increased obviously from 78.10% at 1100 °C to 96.59% at 1350 °C, and reached above 99% at 1400 °C. Not only the thermodynamic conditions, but also kinetic conditions of the reduction for different phases can be notably improved with increasing the coal-based reduction temperature. Since the reaction from Fe^{2+} to Fe is strongly endothermic, the higher the reduction temperature, the more beneficial the quickening of the direct reduction reaction. Additionally, the pyrolysis of coal is intensified with the increase of the temperature, for which the aromatic hydrocarbon and some functional groups can get released and considerable amounts of the tar composition can

appear on the surface of coal granules. As the tar composition contains great quantities of chemical compounds of the tar precursor, a large number of pores can appear after that the volatiles are deposited, which is beneficial to the strengthening of the carbon activity. Meanwhile, the internal diffusion of the reducing gas is enhanced, and the reduction condition is improved. In addition, with increasing the temperature, the oscillation of ions in the lattice of the solid reactant in the equilibrium position is intensified and the displacement phenomenon of those ions occurs because of overcoming the effect of the surrounding ions, which contributes to intensifying the diffusion of ions in the crystal lattice and the crystal chemical reaction at the reaction interface, and the more complete the direct reduction reaction.

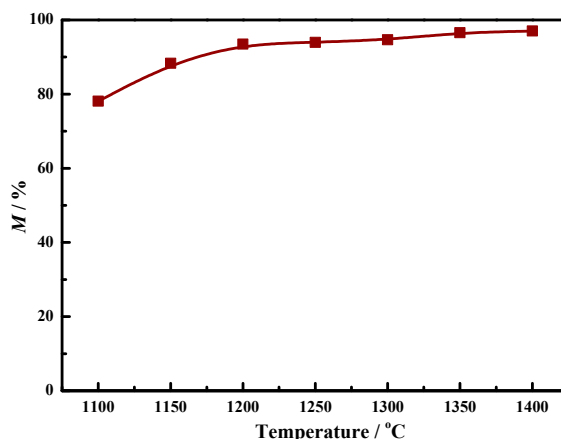
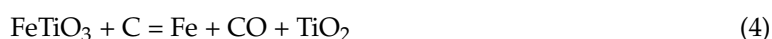


Figure 3. The effect of the temperature on the metallization degree.

3.2. Phase Composition Transformation

In order to study the specific phase compositions at different temperatures and the phase composition transformation of LGVTMP with increasing the reduction temperature, XRD analyses were conducted, with results shown in Figure 4. It is found that the metallic iron, which was predominantly reduced from magnetite and ilmenite with reaction Equations (3) and (4), can be obviously detected in the reduced products.



The incompletely reduced ilmenite can still be found at 1100 °C. When the temperature increased to 1250 °C or above, it was found that the Fe-bearing anosovite ($\text{Fe}_{0.5}\text{Mg}_{0.5}\text{Ti}_2\text{O}_5$) appeared and increased with the increase of the temperature. From the thermodynamic analysis, ferrous pseudobrookite (FeTi_2O_5) can be generated with the reaction Equation (5) at this temperature range:



It is known that the crystal structure of FeTi_2O_5 is not that stable, and the stable temperature is only above 1130 °C. Meanwhile, as the radius difference of magnesium ions (Mg^{2+}) and ferrous iron (Fe^{2+}) are less than 15%, which is in accordance with the forming conditions of isomorphism, the stability of FeTi_2O_5 can be strengthened with the entering of Mg^{2+} into the crystal lattice of FeTi_2O_5 and the replacement of Fe^{2+} [24], contributing to the formation of stable absolute homogenous phases, such as $\text{Fe}_{0.5}\text{Mg}_{0.5}\text{Ti}_2\text{O}_5$, which was found in the reduced phases of coal-based LGVTMP at 1250–1350 °C. Furthermore, the wustite, which was mainly reduced from magnetite and ilmenite, was transformed into magnesium ferrite ($\text{Mg}_{0.77}\text{Fe}_{0.23}\text{O}$) with the replacement of Fe^{2+} with Mg^{2+} in the

reduction process. However, the appearance of Fe-bearing anosovite, like $\text{Fe}_{0.5}\text{Mg}_{0.5}\text{Ti}_2\text{O}_5$, could affect the subsequent separation of Fe-bearing and Ti-bearing phases. From the phase transformation, it was found that the transformation pattern of Mg-bearing phases is $\text{FeTiO}_3 \rightarrow \text{FeTi}_2\text{O}_5 \rightarrow \text{Fe}_{0.5}\text{Mg}_{0.5}\text{Ti}_2\text{O}_5$; ($\text{Fe}_3\text{O}_4/\text{FeTiO}_3 \rightarrow \text{FeO} \rightarrow \text{Mg}_{0.77}\text{Fe}_{0.23}\text{O}$).

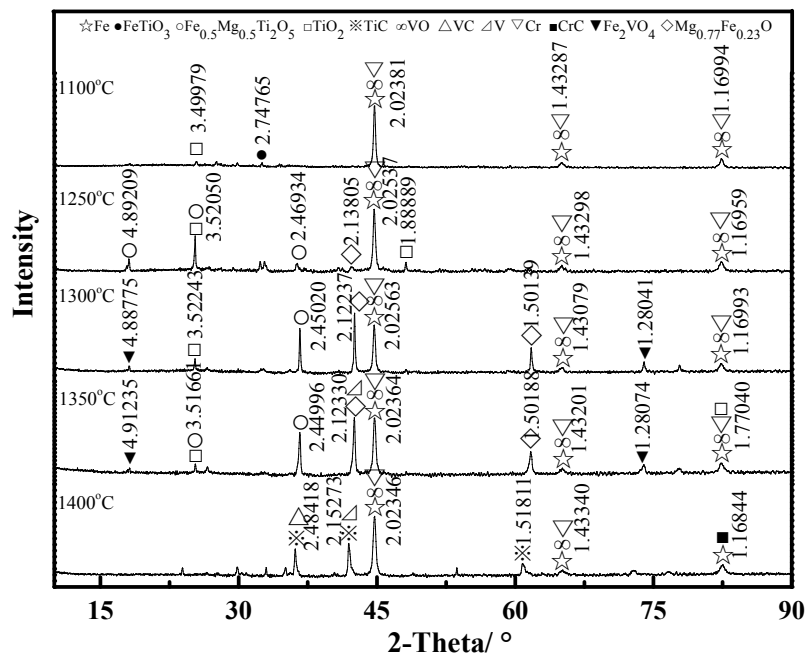


Figure 4. XRD patterns of the reduced LGVTMP at different temperatures.

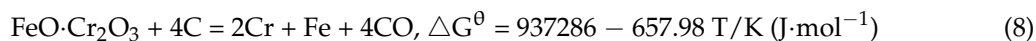
When the temperature reached 1300–1350 °C, the diffraction peaks of $\text{Fe}_{0.5}\text{Mg}_{0.5}\text{Ti}_2\text{O}_5$ was further strengthened in the reduced products, since M_3O_5 -type solid solution (M represents Fe, Mg, and Ti) that was formed by the mutually-soluble ferrous pseudobrookite and anosovite was greatly difficult to be reduced thoroughly [24]. Besides, the trans-V-Fe spinel phase (Fe_2VO_4) was found owing to the reaction Equation (6) of FeO and V_2O_5 in the reduction process above 1270 °C:



On the other hand, vanadium metal just appeared above 1350 °C because the reduction reaction from vanadium oxides to vanadium metal, e.g., Equation (7), is of great difficulty according to thermodynamic analysis:



However, compared with the generated conditions of vanadium metal, chromium metal was much more easily generated with the reaction Equation (8):



When the temperature increased to 1400 °C, carbides of vanadium, titanium, and chromium were found simultaneously, which was also detected in the following microscopic examination, and should be avoided as much as possible. From the phase transformation, it was found that the transformation pattern of V-bearing, Ti-bearing and Cr-bearing phases is $\text{Fe}_2\text{VO}_4 \rightarrow \text{VO} \rightarrow \text{V} \rightarrow \text{VC}$; $\text{FeTiO}_3 \rightarrow \text{FeTi}_2\text{O}_5 \rightarrow \text{TiO}_2 \rightarrow \text{TiC}$; $\text{FeCr}_2\text{O}_4 \rightarrow \text{Cr} \rightarrow \text{CrC}$.

3.3. Microscopic Examination

In above coal-based reduction behavior, basic reduction results and the phase composition transformation have been given, and it is essential to further examine the microstructure of reduced pellets. Figure 5 presents the microstructures of reduced LGVTMP at different temperatures at 5000 \times . It is observed that the amounts of metallic iron particles obviously increased and the accumulation and growing tendency were gradually facilitated evidently with increasing the temperature from 1100 °C to 1400 °C. The metallic iron was generated evenly along some preferential directions at 1100 °C, which was found in the microstructure, and the accumulation and growing percentage were not so large. Additionally, there were still some original titanium-ferrum oxides that were not reduced absolutely, characterized by EDS of area A (see Figure 6a). Figure 5c could be interpreted as clear heavy (iron) compounds in a silicated grassy matrix (dark). The EDS analyses of corresponding areas B and E are shown in Figure 6b,c with increasing the temperature below 1350 °C, and it was revealed that more and more titanium oxides without Fe reduced from ilmenite were found. The coal-based reduction can promote the separation of Ti from Fe, and this is beneficial for improving the element beneficiation rate and utilization efficiency. However, the carbides, especially titanium carbide and the vanadium carbide, with EDS analysis in Figure 6d for the corresponding area F, were generated with continually increasing the temperature to 1400 °C, but this is not necessary as large amounts of reducing coal would be consumed. Thus, the appropriate temperature should be better guaranteed below 1350 °C during coal-based reduction.

It was also found that the vanadium content in the titanium oxides decreased as a whole with increasing the temperature, which could be related to the vanadium content distributed in the metallic iron, and this is in accordance with a previous study where the V content in metallic iron particles increased correspondingly with the appearance of vanadium metal in the range of 1300–1400 °C [4]. The titanium-bearing phases were mostly titanium carbide at 1400 °C, and the V content in titanium-bearing phases was at a very high level because of the local enrichment of vanadium carbides. Therefore, EDS analyses of metallic iron phases were further studied, with results shown in Figure 7, and the V content distributed in the metallic iron ($[V]_{Fe}$) increased at 1300–1400 °C, which is perfectly coincident with the results of the vanadium content decrease in the titanium oxides. Furthermore, the element transformation characteristics were further researched in the latter magnetic separation studies.

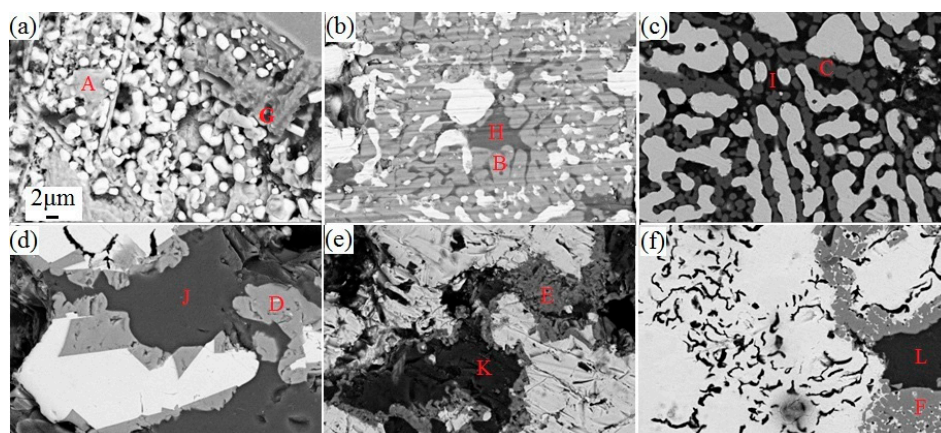


Figure 5. The effect of temperature on the microstructure of reduced LGVTMP at 5000 \times : (a) 1100 °C; (b) 1200 °C; (c) 1250 °C; (d) 1300 °C; (e) 1350 °C; and (f) 1400 °C.

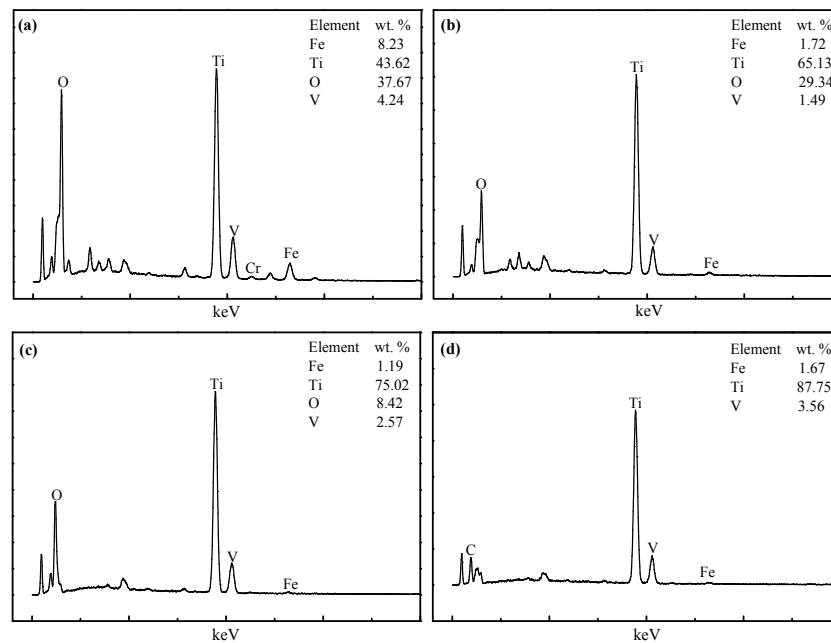


Figure 6. EDS analysis of different light grey areas: (a) area A; (b) area B; (c) area E; and (d) area F.

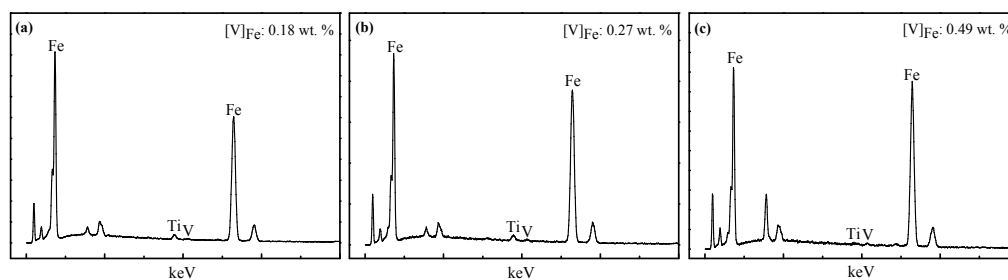


Figure 7. EDS analysis of metallic iron particles: (a) 1300 °C; (b) 1350 °C; and (c) 1400 °C.

By analyzing the black areas H, K, and L, with corresponding results shown in Figure 8b–d, it is found that silicate phases, especially calcium silicate phases, transformed from calcium ferrite that was found at 1100 °C (see area G) with EDS analysis in Figure 8a, were observed and gradually aggregated with the increase in the temperature from 1200 °C to 1350 °C. However, some silicate phases were infiltrated into metallic iron since it appears that chromium carbides, and especially titanium carbides that were also found in the above XRD analysis, could probably contribute to the sintering phenomenon becoming serious at 1400 °C because it is well-known that those carbides with high melting points can increase the viscosity of the metallic iron and the slag, which would result in the hanging and diffusing of the slag in the metallic iron [4,25]. It has also been found that the slag and metallic iron were very difficult to separate from experimental studies of melting separation, thus, magnetic separation was employed to separate the magnetic and non-magnetic products.

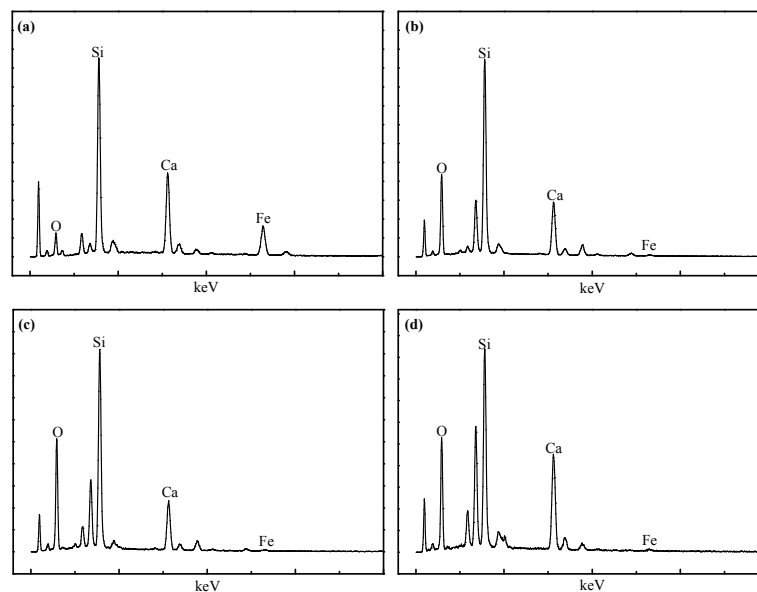


Figure 8. EDS analysis of different areas: (a) area G; (b) area H; (c) area K; and (d) area L.

3.4. Magnetic Separation Behavior

It has been revealed that the nucleation, accumulation, and growth of metallic iron phases were greatly promoted and a large number of large metallic iron beads were formed, especially at relatively higher elevated temperatures from the above SEM examination, which should be beneficial for separating the metallic iron phases and other phases, according to previous studies, by magnetic separation [9]. However, for LGVTM ore, since the resource characteristics and mineral compositions are specific, the magnetic separation also has a significant relationship with other phases, including phases that tended to attach to the metallic iron phase and phases that showed an opposite tendency. Thus, it is important to study the element transformation behavior and the recovery rate of different valuable elements, including Fe, V, Ti, and Cr.

It is well-known that, in a certain range, the increase of the magnetic intensity is beneficial for the entry of high-grade iron-bearing particles to the magnetic products, which can contribute to the grade and weight of magnetic products. Thus, the iron recovery rate increased. However, the continuous increase of the magnetic intensity is beneficial for the entry of low-grade iron-bearing particles to the magnetic products, for which the magnetic products increased, but the grade of magnetic products decreased, which was reversely beneficial for the iron recovery rate. In order to investigate the effect of the temperature on the element transformation and the recovery rate, proved appropriate magnetic intensity of $160 \text{ kA} \cdot \text{m}^{-1}$, was adopted. Typical results of the iron recovery rate, which was calculated according to Equation (9):

$$\eta_{Fe} = \frac{TFe_M \times m_M}{TFe_R \times m_R} \times 100\% \quad (9)$$

where η_{Fe} is the iron recovery rate (%), TFe_M is the grade of magnetic products (%), TFe_R is the grade of reduction products (%), m_M is the mass of magnetic products (g), and m_R is the mass of reduced products used for the magnetic separation (g), which were shown in Figure 9 on the basis of analyzing TFe values of the reduced products and the magnetic products. Typical chemical compositions of reduced products at $1350 \text{ }^\circ\text{C}$, and the corresponding magnetic and non-magnetic products, are presented in Table 3. It is found that the grade of the reduced product increased as a whole from $1100 \text{ }^\circ\text{C}$ to $1400 \text{ }^\circ\text{C}$, while that of the magnetic products increased to high values at $1300\text{--}1350 \text{ }^\circ\text{C}$ and then decreased at $1400 \text{ }^\circ\text{C}$. By calculating the different values of the reduced products and magnetic-separation products, it was observed that the iron recovery rate increased from 86.27% at $1100 \text{ }^\circ\text{C}$ to 91.49% at $1350 \text{ }^\circ\text{C}$, but then quickly decreased to 83.70% at $1400 \text{ }^\circ\text{C}$.

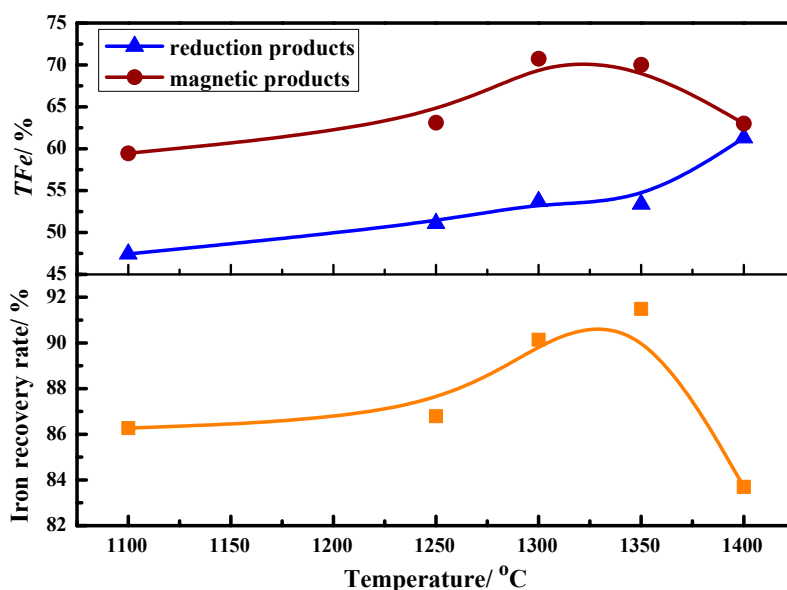


Figure 9. The grade of the reduced products and magnetic products and iron recovery rate at different temperatures.

Table 3. Chemical compositions of reduced LGVTMP at 1350 °C and the corresponding magnetic and non-magnetic products after magnetic separation (wt %).

Item	TFe	MFe	V	TiO ₂	Cr ₂ O ₃
Reduced Products	53.38	51.56	1.06	24.62	0.18
Magnetic Products	70.01	62.59	1.04	19.67	0.19
Non-Magnetic Products	-	-	1.04	34.32	0.12

The metallic iron grains were relatively smaller and significantly mingled with the gangue phases at lower temperature, which makes it impossible for the metallic iron grains and gangue phases to realize effective dissociation. The iron oxides were partially reduced into the metallic iron, and the mingled gangue phases affected the magnetic performance of metallic iron particles, contributing to the lower iron recovery rate at lower temperature. Since both the size of metallic iron grains and *TFe* values of reduced products increased and the mingled phenomenon of the metallic iron grains and gangue phases were lowered by increasing the reduction temperature, the iron recovery rate reached a relatively higher value of 91.49% at 1350 °C. It is observed that the size of certain metallic iron grains reached above 100 μm at 1350 °C, and the gangue phases mingled in the metallic iron were quite few, so when the grinding fineness was lower than 0.074 mm, with the gained relatively purer gangue particles and high-grade iron-bearing particles, a relatively higher iron recovery rate was obtained after magnetic separation. Consequently, it could be concluded that the iron recovery rate increased through the magnetic separation due to the decrease of the mingled extent of the metallic iron and gangue phases, which was caused by the increase of the reduction temperature, which is beneficial for increasing the size of the metallic iron grains and decreasing the mingled extent. However, due to the overreduction, considerable amounts of carbides especially TiC, CrC, and VC appeared with increasing the temperature from 1350 °C to 1400 °C, which have been revealed in the XRD pattern in Figure 4. Part of these carbides was distributed in the metallic iron phases, so the magnetic performance of magnetic phases was lowered, leading to the evident decrease of the iron recovery rate.

It is well-known that the reduction temperature also has a significant relationship with the transformation behavior of valuable V, Ti, and Cr, in addition to Fe, and the effects of temperature on the regular transformation pattern of V, Ti, and Cr was further studied, with typical results exhibited in Figure 10, in which $Cr_M\%$ represents the recovery rate of Cr in magnetic products, and $V_M\%$ represents

that of V in magnetic products. $Ti_N\%$ represents the recovery rate of Ti in non-magnetic products, and $Ti_M\%$ represents that of Ti in magnetic products. $Cr_M\%$, $V_M\%$, $Ti_N\%$ and $Ti_M\%$ were calculated according to Equations (10)–(13):

$$Cr_M\% = \frac{Cr_M \times m_M}{Cr_R \times m_R} \times 100\% \quad (10)$$

$$V_M\% = \frac{V_M \times m_M}{V_R \times m_R} \times 100\% \quad (11)$$

$$Ti_N\% = \frac{Ti_N \times m_N}{Ti_R \times m_R} \times 100\% \quad (12)$$

$$Ti_M\% = 1 - Ti_N\% \quad (13)$$

where Cr_M is the mass percent of Cr in magnetic products (%), Cr_R is the mass percent Cr in reduced products (%), V_M is the mass percent of V in magnetic products (%), V_R is the mass percent of V in reduced products (%), Ti_N is the mass percent of Ti in non-magnetic products (%), Ti_M is the mass percent of Ti in non-magnetic products (%), m_N is the mass of non-magnetic products (g), and Ti_R is the mass percent Ti in reduced products (%). It was found that the percent of V that transformed into the magnetic products decreased from 55.93% at 1100 °C to 49.76% at 1300 °C and then increased to 79.26% at 1400 °C in the magnetic separation process. Below 1300 °C, owing to the weak magnetic intensity of vanadium oxides or V-Fe oxides, these oxides did not specifically transform into magnetic products or non-magnetic products, and probably tended slightly to transform into non-magnetic products with an increase in the temperature. However, since it has been reported that vanadium metal was easily distributed in the metallic iron phases with the increasing appearance of vanadium metal above 1300 °C [1,4], the rate of vanadium that transformed into the magnetic products increased. The percent of Cr that transformed into the magnetic products increased from 56.03% at 1100 °C to above 90% at 1400 °C. From the phase composition of reduced products, chromium metal was detected at lower temperatures and the generated amounts increased with the increase in the temperature. Additionally, similar to vanadium metal, chromium metal was also easily distributed in metallic iron phases, and this is coincident with the typical result of Cr transformation behavior [1,4,25]. The percent of Ti that transformed into the non-magnetic products ($Ti_N\%$) increased from 40.70% at 1100 °C to 50.44% at 1300 °C and 49.56% at 1350 °C as the reduction of titanium oxides from titanium-ferrum oxides increased and separated from the generated metallic iron. However, $Ti_N\%$ decreased to 26.37% at 1400 °C, as large quantities of titanium carbides appeared and were distributed in the mingled slag-iron phases that were difficult to separate, as it has been reported that TiC has a specific adverse function in the separation of the metallic iron and the slag during smelting [4]. Through the magnetic separation of coal-based reduced products, it was demonstrated that, on one hand, the transforming percent of Ti into the non-magnetic products (49.56%) was relatively higher at 1350 °C, especially the transformation percent of Cr and V into the magnetic products was relatively higher (V: 68.44%; Cr: 73.63%); thus the separation of Cr, V, and Ti can be preliminarily realized after magnetic separation for the reduced products. On the other hand, the transforming percent of Ti, Cr, and V into the magnetic products (Ti: 73.63%, V: 79.26%; Cr: 90.00%) was relatively higher at 1400 °C, thus the separation of Cr, V, Ti, and non-magnetic phases can be preliminarily realized.

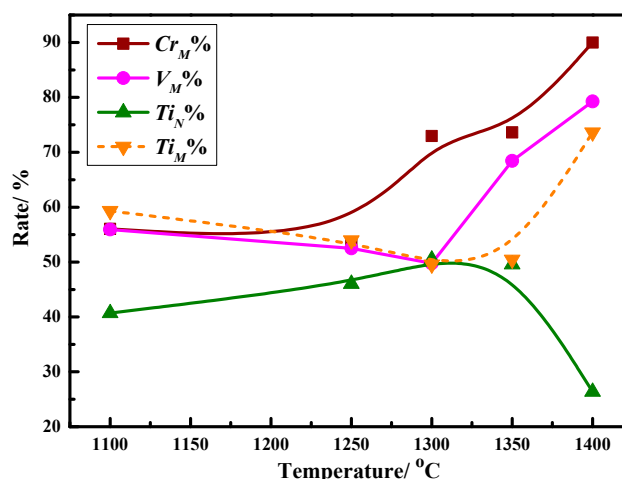


Figure 10. The effect of temperature on the transformation patterns of V, Ti, and Cr.

4. Conclusions

Coal-based reduction and magnetic separation behavior of LGVTMP were investigated in the present work. From the studies carried out, following conclusions can be drawn:

1. Different kinds of metallized pellets were obtained after the coal-based reduction of LGVTMP with appropriate C/O. It is found that the metallization degree increased obviously with increasing the temperature from 1100 °C to 1400 °C.
2. From the characterization and analysis of XRF, ICP-AES, XRD, SEM, and EDS, it is observed that the amounts of metallic iron particles obviously increased and the accumulation and growing tendency were gradually facilitated with the increase in the temperature from 1100 °C to 1400 °C. It is also found that the titanium oxides were gradually reduced and separated from titanium-ferrum oxides during reduction. In addition, silicate phases, especially calcium silicate phases, transformed from calcium ferrite at 1100 °C, were observed, and gradually aggregated with the increase in the temperature from 1200 °C to 1350 °C, but some silicate phases infiltrated into metallic iron at 1400 °C, as it appears that carbides, especially TiC, could probably contribute to the sintering phenomenon becoming serious.
3. From the comprehensive study, it was obtained that the transformation behavior for valuable elements was as follows: $Fe_2VO_4 \rightarrow VO \rightarrow V \rightarrow VC$; $FeTiO_3 (\rightarrow FeTi_2O_5) \rightarrow TiO_2 \rightarrow TiC$; $FeCr_2O_4 \rightarrow Cr \rightarrow CrC$; $FeTiO_3 (\rightarrow FeTi_2O_5) \rightarrow Fe_{0.5}Mg_{0.5}Ti_2O_5$; $(Fe_3O_4/FeTiO_3 \rightarrow) FeO \rightarrow Mg_{0.77}Fe_{0.23}O$.
4. Through the magnetic separation of reduced products, it is demonstrated that the separation of Cr, V, Ti, and non-magnetic phases can be preliminarily realized.

Acknowledgments: The authors are especially thankful to National Project Support Program of China (grant No. 2015BAB19B02) and 973 Program (grant No. 2013CB632603).

Author Contributions: Gongjin Cheng and Xiangxin Xue conceived and designed the experiments. Gongjin Cheng, Zixian Gao and Xiangxin Xue performed the experiments and analyzed the data. He Yang provided sample material and contributed to the interpretation. Gongjin Cheng and Xiangxin Xue took the lead in writing the main manuscript and Mengyang Lv helped to check the manuscript. All authors contributed to the final manuscript version.

Conflicts of Interest: The authors declare no conflict of interest.

References

1. Du, H.G. *Principle of Smelting Vanadium-Titanium Magnetite in the Blast Furnace*, 1st ed.; Science Press: Beijing, China, 1996; pp. 1–20.
2. Wang, X.Q. *Smelting of Vanadium-Titanium Magnetite in the Blast Furnace*, 1st ed.; Metallurgical Industry Press: Beijing, China, 1994; p. 1.
3. Li, H.M.; Wang, R.J.; Xiao, K.Y.; Zhang, X.H.; Liu, Y.L.; Sun, L. Characteristics and current utilization status of ultra-low-grade magnetite resource, and suggestion on its exploration and development. *Geol. Bull. China* **2009**, *28*, 85–90.
4. Cheng, G.J.; Xue, X.X.; Jiang, T.; Duan, P.N. Effect of TiO₂ on the crushing strength and smelting mechanism of high chromium vanadium-titanium magnetite pellets. *Metall. Mater. Trans. B* **2016**, *47*, 1713–1726. [[CrossRef](#)]
5. Cheng, G.J.; Liu, J.X.; Liu, Z.G.; Chu, M.S.; Xue, X.X. Non-isothermal reduction kinetics and mechanism of high chromium vanadium-titanium magnetite pellets. *Ironmak. Steelmak.* **2015**, *42*, 17–26. [[CrossRef](#)]
6. Liu, J.X.; Cheng, G.J.; Liu, Z.G.; Chu, M.S.; Xue, X.X. Reduction process of pellet containing high chromic vanadium-titanium magnetite in cohesive zone. *Steel Res. Int.* **2015**, *86*, 808–816. [[CrossRef](#)]
7. Zhou, M.; Yang, S.T.; Jiang, T.; Xue, X.X. Influence of Basicity on High-Chromium Vanadium-Titanium Magnetite Sinter Properties, Productivity, and Mineralogy. *JOM* **2015**, *67*, 1203–1213. [[CrossRef](#)]
8. Sun, H.Y.; Dong, X.J.; She, X.F.; Xue, Q.G.; Wang, J.S. Solid state reduction of titanomagnetite concentrate by graphite. *ISIJ Int.* **2013**, *53*, 564–569. [[CrossRef](#)]
9. Chen, S.Y.; Chu, M.S. Metalizing reduction and magnetic separation of vanadium titanomagnetite based on hot briquetting. *Int. J. Miner. Metall. Mater.* **2014**, *21*, 225–233. [[CrossRef](#)]
10. Jiang, T.; Wang, S.; Guo, Y.F.; Chen, F.; Zheng, F.Q. Effects of basicity and MgO in slag on the behaviors of smelting vanadium titanomagnetite in the direct reduction-electric furnace process. *Metals* **2016**, *6*, 107–121. [[CrossRef](#)]
11. Yu, W.; Sun, T.; Cui, Q.; Xu, C.; Kou, J. Effect of coal type on the reduction and magnetic separation of a high-phosphorus oolitic hematite ore. *ISIJ Int.* **2015**, *55*, 536–543. [[CrossRef](#)]
12. Kasai, E.; Mae, K.; Saito, F. Effect of mixed-grinding on reduction process of carbonaceous material and iron oxide composite. *ISIJ Int.* **1995**, *35*, 1444–1451. [[CrossRef](#)]
13. Nascimento, R.C.; Mourao, M.B.; Capocchi, J.D.T. Microstructures of Self-reducing Pellets Bearing Iron Ore and Carbon. *ISIJ Int.* **1997**, *37*, 1050–1056. [[CrossRef](#)]
14. Yu, W.; Sun, T.; Liu, Z.; Kou, J.; Xu, C. Effects of particle sizes of iron ore and coal on the strength and reduction of high phosphorus oolitic hematite-coal composite briquettes. *ISIJ Int.* **2014**, *54*, 56–62. [[CrossRef](#)]
15. Sun, Y.S.; Han, Y.X.; Gao, P.; Ren, D.Z. Distribution behavior of phosphorus in the coal-based reduction of high-phosphorus-content oolitic iron ore. *Int. J. Miner. Metall. Mater.* **2014**, *21*, 331–338. [[CrossRef](#)]
16. Gao, P.; Li, G.F.; Han, Y.X.; Sun, Y.S. Reaction behavior of phosphorus in coal-based reduction of an oolitic hematite ore and pre-dephosphorization of reduced iron. *Metals* **2016**, *6*, 82. [[CrossRef](#)]
17. Inaba, S. Overview of new direct reduced iron technology. *Tetsu-to-Hagane* **2001**, *87*, 221–227. [[CrossRef](#)]
18. Zhu, D.; Mendes, V.; Chun, T.; Pan, J.; Li, Q.; Li, J.; Qiu, G. Direct reduction behaviors of composite binder magnetite pellets in coal-based grate-rotary kiln process. *ISIJ Int.* **2011**, *51*, 214–219. [[CrossRef](#)]
19. Jiang, X.; Liu, S.; Huang, T.; Zhang, G.; Guo, H.; Shiao, G.H.; Shen, F.M. Effects of reducing time on metallization degree of carbothermic reduction of tall pellets bed. *ISIJ Int.* **2016**, *56*, 88–93. [[CrossRef](#)]
20. Jung, S.M. Effects of CaO/CaCO₃ on the carbothermic reduction of titanomagnetite ores. *Metall. Mater. Trans. B* **2015**, *46*, 1162–1174. [[CrossRef](#)]
21. Jung, S.M. Effects of the content and particle size of char in the composite on the carbothermic reduction of titanomagnetite at 1100 °C. *ISIJ Int.* **2014**, *54*, 2933–2935. [[CrossRef](#)]
22. Jung, S.M. Evaluation of reduction progress of raw titanomagnetite and char composite by thermogravimetry. *ISIJ Int.* **2013**, *53*, 1487–1489. [[CrossRef](#)]
23. Hu, T.; Lv, X.W.; Bai, C.G.; Lun, Z.G.; Qiu, G.B. Carbothermic reduction of titanomagnetite concentrates with ferrosilicon addition. *ISIJ Int.* **2013**, *53*, 557–563. [[CrossRef](#)]

24. Yu, S. Research on the Solid-Phase Enhancement Reduction and Magnetic Separation of Vanadium Titanomagnetite. Master's Thesis, Northeastern University, Shenyang, China, 2013.
25. Cheng, G.J.; Xue, X.X.; Gao, Z.X.; Jiang, T.; Yang, H.; Duan, P.N. Effect of Cr_2O_3 on the reduction and smelting mechanism of high-chromium vanadium-titanium magnetite pellets. *ISIJ Int.* **2016**, *56*, 1938–1947. [[CrossRef](#)]



© 2017 by the authors. Licensee MDPI, Basel, Switzerland. This article is an open access article distributed under the terms and conditions of the Creative Commons Attribution (CC BY) license (<http://creativecommons.org/licenses/by/4.0/>).